Biogeosciences, 12, 2893–2905, 2015
www.biogeosciences.net/12/2893/2015/
doi:10.5194/bg-12-2893-2015


Biogeosciences Open Access

# Modeling forest lines and forest distribution patterns with remote-sensing data in a mountainous region of semiarid central Asia

**M. Klinge**[1], **J. Böhner**[2], **and S. Erasmi**[1]

[1]Institute of Geography, University of Göttingen, Goldschmidtstr. 5, 37077 Göttingen, Germany
[2]Institute of Geography, University of Hamburg, Bundesstraße 55, 20146 Hamburg, Germany

*Correspondence to:* M. Klinge (mklinge1@gwdg.de)

Received: 17 July 2014 – Published in Biogeosciences Discuss.: 13 October 2014
Revised: 19 April 2015 – Accepted: 21 April 2015 – Published: 20 May 2015

**Abstract.** Satellite images and digital elevation models provide an excellent database to analyze forest distribution patterns and forest limits in the mountain regions of semiarid central Asia on the regional scale. For the investigation area in the northern Tien Shan, a strong relationship between forest distribution and climate conditions could be found. Additionally areas of potential human impact on forested areas are identified at lower elevations near the edge of the mountains based on an analysis of the differences in climatic preconditions and the present occurrence of forest stands.

The distribution of spruce (*Picea schrenkiana*) forests is hydrologically limited by a minimum annual precipitation of 250 mm and thermally by a minimum monthly mean temperature of 5 °C during the growing season. While the actual lower forest limit increases from 1600 m a.s.l. (above sea level) in the northwest to 2600 m a.s.l. in the southeast, the upper forest limit rises in the same direction from 1800 m a.s.l. to 2900 m a.s.l.. In accordance with the main wind directions, the steepest gradient of both forest lines and the greatest local vertical extent of the forest belt of 500 to 600 m to a maximum of 900 m occur at the northern and western mountain fronts.

The forests in the investigation area are strongly restricted to north-facing slopes, which is a common feature in semiarid central Asia. Based on the presumption that variations in local climate conditions are a function of topography, the potential forest extent was analyzed with regard to the parameters slope, aspect, solar radiation input and elevation. All four parameters showed a strong relationship to forest distribution, yielding a total potential forest area that is 3.5 times larger than the present forest remains of 502 km$^2$.

## 1 Introduction

The latitudinal and elevational variation in distinct plant associations and geomorphologic landscape units has been used for a long time to deduce regional environmental and climatical conditions in geosciences (e.g., von Humboldt, 1845–1862; Troll, 1973a, b; Hövermann, 1985). Image classification and GIS modeling of remote-sensing data are standard methods to map landscape elements and their distribution in remote areas, which are poorly accessible due to logistic or political difficulties. Satellite analysis based on automated image processing offers a quick and useful alternative to field mapping or manual digitalization from aerial images (Mayer and Bussemer, 2001). While satellite images such as Landsat data provide excellent information to delineate the spatial forest distribution (Hansen et al., 2013), SRTM (Shuttle Radar Topography Mission) data can be used to examine relief-dependent distribution patterns with a digital terrain model (DTM). The combination of these two data sets enables high-resolution mapping on a regional to local scale.

The geoecologic and climatic environmental settings control the natural distribution of forest stands (Holtmeier, 2000; Körner, 2012; Miehe et al., 2003). In addition, the actual situation can strongly be influenced by human activities such as logging, fire clearing and animal grazing, which decreases the potential natural forest area (PFA). This often makes it difficult to differentiate between natural factors and human impact on the distribution of timbered areas. In general, human activity has reduced the forest area since prehistorical times so that the actual forest area (AFA) pattern mostly represents the minimum of the potential environmental dis-

tribution range. However, due to the possibility of anthropogenic forest management and afforestation during the last centuries, forests may occur at sites less favorable for natural tree growth.

Due to the highly continental, cold and semiarid climate in central Asia, tree growth is mostly determined by topography parameters. Forest stands beyond sites with more favorable conditions regarding groundwater are predominantly limited to north-facing slopes in the mountains with an upper and lower forest limit (Dulamsuren et al., 2014; Hilbig, 1995; Klinge et al., 2003; Treter, 1996, 2000).

Different definitions have been used for tree and forest lines (Körner, 2012; Körner and Paulsen, 2004). The treeline ecotone covers three main boundary lines at the upper limit of forest distribution. The highest is the tree species line, where tree seedlings occur but no adult trees. The treeline is the maximum elevation where patches of forest can exist at topographically favorable places. In our investigation we refer to the forest line, which is defined as the limit of closed forest at the upper (timberline) and lower boundary of forest distribution.

For the region of the northern Tien Shan in China, Dai et al. (2013) state an upper forest line beginning with 2900 m a.s.l. in the west, which decreases eastward down to 2500 m a.s.l. and then rises again to 2900 m a.s.l. in the east. In the northwestern Tien Shan, Fickert (1998) reports an upper forest line of 2900 and 2850 m a.s.l. and a lower forest line of 2400 and 2500 m a.s.l., respectively for the Sailijski-Alatau and Kungeij-Alatau. In the Altai Mountains, Klinge et al. (2003) found upper forest lines increasing eastward from 1800 to 2600 m a.s.l. and, concurrently, lower forest lines increasing from 1000 to 2200 m a.s.l., while the vertical extension of the forest belt varies between 400 and 1200 m.

Tree growth in high mountains is generally restricted by temperature conditions (Haase et al., 1964; Holtmeier, 2000; Jobbagy and Jackson, 2000; Körner, 2012). The upper forest line is a thermally determined distribution boundary that is generally defined by the mean July temperature (Walter and Breckle, 1994) or the warmest-month isotherm of 10 °C. According to Körner (2012) and Körner and Paulsen (2004), this parameter is not appropriate for all parts of the world. This can be seen in Fickert (1998), who shows that the upper forest line in the northern Tien Shan coincides well with the 10 °C July isotherm, while further south in the northwestern Himalaya and northwestern Karakorum, it is connected to the July isotherms of 16 and 12 °C, respectively. For the eastern side of the northern Tien Shan, Dai et al. (2013) report a mean temperature of the warmest month of 10.5 °C at the mean position of the alpine forest line. Moreover, the mean annual air temperature (MAAT) is weakly correlated to the forest line because it includes temperatures from the nongrowing season, which play a minor role in tree growth (Jobbagy and Jackson, 2000; Körner, 2012).

A suitable way of describing the temperature environment at the upper forest line is by using a minimum threshold value for the mean air temperature during the growing season, which is defined as the period of monthly mean temperatures above 5 °C (Dai et al., 2013; Körner, 2012; Körner and Paulsen, 2004). Based on the strong correlation between soil and air temperatures, Körner and Paulsen (2004) state a global range of 5.5 to 7.5 °C for minimum mean air temperatures during the growing season. Paulsen and Körner (2014) developed a climate-based model for treeline prediction by defining the growing season as days with a mean temperature above 0.9 °C and a mean temperature of more than 6.4 °C during that time. For the upper forest line between 2750 and 2920 m a.s.l. in the Tien Shan in Kyrgyzstan Körner (2012) found a mean temperature of 6.5 °C during the 155 days of the growing season (late April until late September).

The forest expansion into dry regions is controlled by precipitation and soil water supply (Dulamsuren et al., 2010, 2014; Kastner, 2000; Klinge et al., 2003). Between the more humid mountain regions and the arid basins of central Asia, a lower limit of forest distribution occurs, which is termed the lower forest line. According to Walter and Breckle (1994) this forest distribution boundary coincides with an annual precipitation of at least 300 mm, while Holdridge (1947) proposes 250 mm and Miehe et al. (2003) found *Juniperus* trees in southern Tibet growing in regions with an annual precipitation of between 200 and 250 mm. Dulamsuren et al. (2010) state an annual precipitation between 230 and 400 mm at lower elevations for larch forests in northern and central Mongolia. In western Mongolia Dulamsuren et al. (2014) found coniferous forests existing at an annual precipitation of around 120 mm, which are explained by soil water benefits due to the occurrence of permafrost ice in the soil.

Everywhere in mountainous areas of the semiarid inner-Asian forest steppe coniferous forests are restricted to north-facing slopes. While the north-facing slopes are dominated by larch trees *(Larix sibirica)* in Mongolia, spruce trees *(Picea schrenkiana)* occur in the Tien Shan (Dai et al., 2013; Fickert, 1998; Liu et al., 2013; Wang 2005, 2006). Thus, the restriction of conifers to north-facing slopes in the inner-Asian forest steppe is not bound to certain tree species but rather to the environmental settings.

The semiarid climate conditions generate an overall deficiency of moisture which considerably influences the elevational forest distribution and may even control the upper forest limit (Liang et al., 2012; Liu et al., 2013; Miehe et al., 2008). A specific relief position is combined with particular climate conditions such as temperature, precipitation, evaporation and insulation, which are similar at comparable sites in the surroundings. For this reason the relief parameters elevation, aspect, slope angle and solar radiation input can be used to define topoclimatic conditions in mountain regions (Miehe et al., 2003). However, to identify potential forest sites based on those definitions, the geologic and soil properties have to be comparable.

The impact of human activity on vegetation and especially on the forest since prehistorical times is a permanent question


**Figure 1.** Map overview showing the investigation area detailed (trapezoid) in central Asia.

that needs to be investigated to clarify the environmental significance of any actual forest line (Miehe and Miehe, 2000). Dulamsuren et al. (2014) found a considerable anthropozoogenic influence on the actual lower forest line in the Mongolian Altai. For northern Mongolia, Schlütz et al. (2008) showed that the present vegetation pattern in the mountain taiga where steppes occur on south-facing slopes is caused by climate conditions and relief and does not originate from human activities.

Human impact on natural forests in Kazakhstan goes back to prehistoric times, with nomadism and animal grazing as a way of life adapted to the natural environmental conditions of the steppe (Karger, 1965; Giese, 1981, 1983). During summertime the alpine meadows and mountain steppes in the upper mountains were regularly used as pastures for the livestock. Even during Soviet times in Kazakhstan the nomadic movements were generally adopted by the sovkhoz system. Even today the alpine pastures are still in use. Extensive animal grazing prevents the rejuvenation of trees, and nomads may expand the grassland by setting fire to it.

Spatial models, which are able to predict the climatically induced forest distribution and especially the upper forest line on a global scale by exclusively using spatial climate data, already exist (Paulsen and Körner, 2014). However, a clear method to empirically distinguish the actual forest distribution and its elevational limits for small areas covering a single mountain system and to simultaneously investigate the potential human impact is lacking. In this investigation we introduce a procedure to solve this problem based on medium-resolution remote-sensing data. In addition, spatially explicit climate data and tree-growth-limiting climate parameters serve to differentiate potential human impact from natural conditions in the forest distribution.

## 2 Study area

The investigation area detailed, Uzynkara Ridge, also known as the Ketmen Mountain range, the Ketmen Mountain range, is located in the northernmost part of the Tien Shan in central Asia on the border between Kazakhstan and China (79–81° E/42°45′–43°45′ N) (Fig. 1). This closed mountain system was chosen for investigation because it provides excellent topographic preconditions to clearly indicate the lower and upper boundaries of forest distribution between the middle and central part of Asia. It fills a knowledge gap about forest lines between regions of the Tien Shan in the south and east, and the Altai mountains in the north (Fickert, 1998; Dai et al., 2013; Klinge et al., 2003). The main cities in the region are Shonzy and Kegen. The complete mountain range is part of the catchment area (CA) of the Ili River in the north. While the northern mountain side is directly drained to the Ili River, the Kegen River in the southern intermountain basin first flows westward and then, turning into the Sharyn River, flows in a northerly direction, and the Tekes River in the southernmost part runs eastward into Chinese territory. The mountain system is structured by two main ridges – a northern front range (NFR) and a southern mountain range (SMR) – which converge in the east and enclose an intermountain basin in the west. The highest peak is the Nebesnaja, reaching 3652 m a.s.l. A high mountain plateau at ∼ 3400 m a.s.l. drops southward, while the north-facing slopes are cut steeply by Pleistocene cirques. Today, no glaciation but permafrost occurs in the uppermost areas.

The edge of the mountains is tectonically clearly distinguished from the alluvial fans and fanglomerates at approximately 1500 m a.s.l. in the north and at 2000 m a.s.l. in the southern intermountain basin, following west to east trending fault lines. The mountains mainly consist of metamorphic and volcanic Carboniferous and Devonian rocks, including several Palaeozoic granite bodies. Permian, Silurian and Jurassic rocks are also distributed locally.

The MAAT in Almaty (848 m a.s.l.) is 8.7 °C and in Karakol (1744 m a.s.l.), which is situated south of the investigation area, 6.3 °C (Fickert, 1998). According to Medeu (2010) the mean air temperature is between −8 and −10 °C in January and between 20 and 24 °C in July. In wintertime the Siberian anticyclone produces weather conditions with cold air masses in the basins and warmer air temperatures above the inversion layer between 1000 and 1550 m a.s.l. (Giese, 1973).

The majority of precipitation in Kazakhstan comes with air masses from the west and southwest. In the mountains of the northern Tien Shan, mainly convective rainfall occurs in spring and autumn. Additionally, cold air masses from northern directions bring precipitation to the northern Tien Shan in summertime (Böhner, 2006; Lydolph, 1977). According to Giese (1973) the annual precipitation in the basins of the foreland lies between 100 and 300 mm; in the lower mountains and in the intermountain basin, it is between 300 and

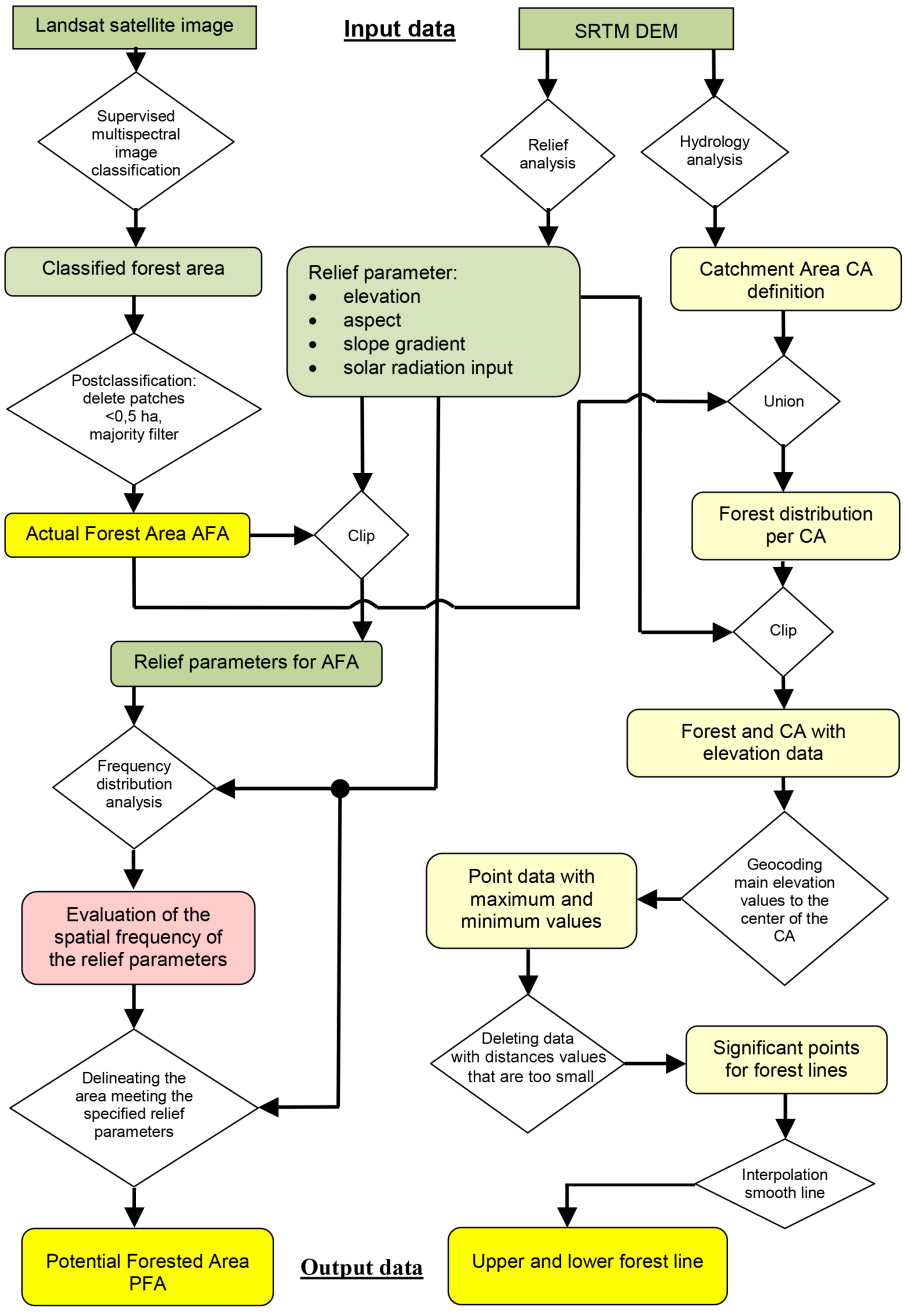


**Figure 2.** Workflow of DEM (digital elevation model) and satellite image processing to determine the spatial forest distribution patterns in semiarid mountain systems of central Asia on a high-resolution scale.

400 mm. In the mountains it increases to more than 800 mm. The precipitation maxima occur in May and June, with a minor, secondary maximum in September.

The foreland, basins and treeless mountain areas are covered by steppe vegetation with forb and bunch grass (Medeu, 2010). In the drier regions to the north, it changes to grassland, sagebrush desert, saltwort and sedge vegetation. The forest belt mainly consists of spruce trees (*Picea schrenkiana*). In the westernmost part, aspen trees (*Populus tremula*) and in the northeastern part birch trees (*Betula pendula*) also occur. On the southern slopes shrub areas also exist.

The soils are distributed according to the climate conditions and the vegetation zones (Medeu, 2010). In the foreland, desert soils occur. In the lower front ranges and in the intermountain basin, mountain steppe soils of castanozem and chernozem type are distributed. In the forest belt dark chernozems, which are locally bleached and podzolized, oc-

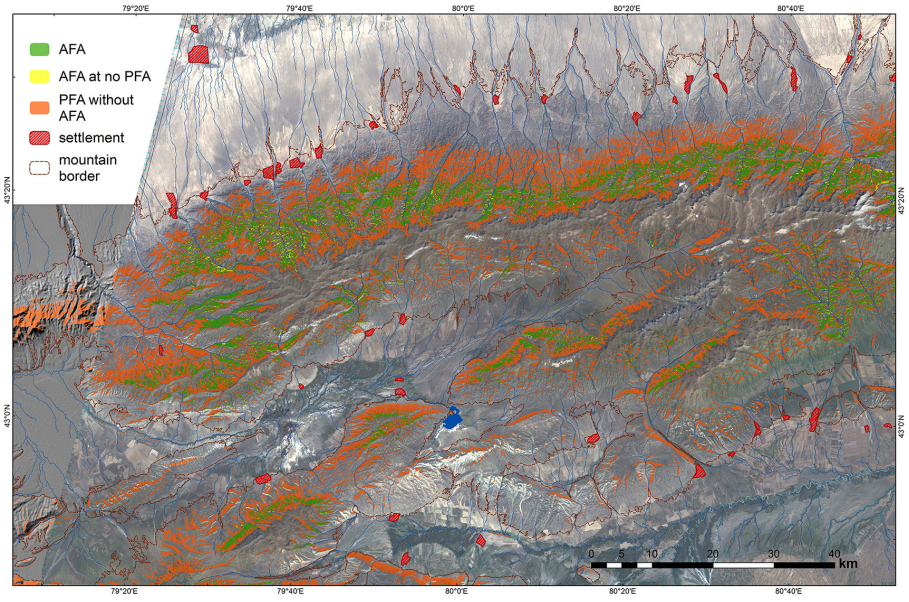


**Figure 3.** Spatial distribution of actual forested area (AFA) and potential forest area (PFA) in the mountainous region of the northernmost Tien Shan shown above a true-color composite of a Landsat 7 satellite image from the 13 September 2000.

**Table 1.** Confusion matrix showing the accuracy report of the supervised maximum likelihood classification (area in ha).

| Reference data | Classification data | | Sum reference | Producer's accuracy | Omission error |
|---|---|---|---|---|---|
| | Forest | No forest | | | |
| Forest | 2696.7 | 333.6 | 3030.3 | 0.890 | 0.110 |
| No forest | 14.7 | 76 426.2 | 76 440.9 | 0.9998 | |
| Sum classification | 2711.4 | 76 759.8 | Total Sum of | Overall | |
| User's accuracy | 0.995 | 0.995 | test data | accuracy | |
| Commission error | 0.0054 | | 79 471.2 | 0.996 | |

cur in forests, and pheaozem soils exist at meadow steppe sites. At high elevations, alpine and subalpine soils occur in mountain meadows and meadow steppes.

Arable land in eastern Kazakhstan is located at the foot of the mountain ranges on the alluvial fans in the basins and on the foothills at a lower elevation. In this transition zone between the pediments and mountain ranges, the soils are improved by a certain amount of Pleistocene loess (Giese, 1983; Karger, 1965; Machalett et al., 2006). After leaving the mountains, the water from the rivers is used for irrigation cultivation on the pediments. In the foothills agriculture is supported by sufficient rainfall; this is the so-called *bogar* cultivation (Giese, 1983). According to these requirements the settlements are located along the main valleys at the mountain boundary. Around the settlements, there is significant woodcutting for construction and fuel.

## 3 Methods

A schematic workflow of the GIS analysis procedure with input data, intermediate data and output data is presented in Fig. 2. The analysis is divided into two main processes: the first is working on the relief parameters to estimate the PFA and the second conducts the delineation of the upper and lower forest lines. The forest lines are defined as the distribution boundaries of closed forest stands with areas larger than 0.5 ha, disregarding single trees, which may represent special environmental places or remnants of former forests. Trees near the rivers in the valley bottoms were excluded from the examination because these are sites which have more favorable conditions regarding groundwater and which are mostly occupied by deciduous trees.

The determination of the AFA in the investigation area was achieved based on a supervised maximum likelihood classification from multispectral satellite images (visible light and infrared channels) of Landsat 7/ETM+ from the 13 Septem-

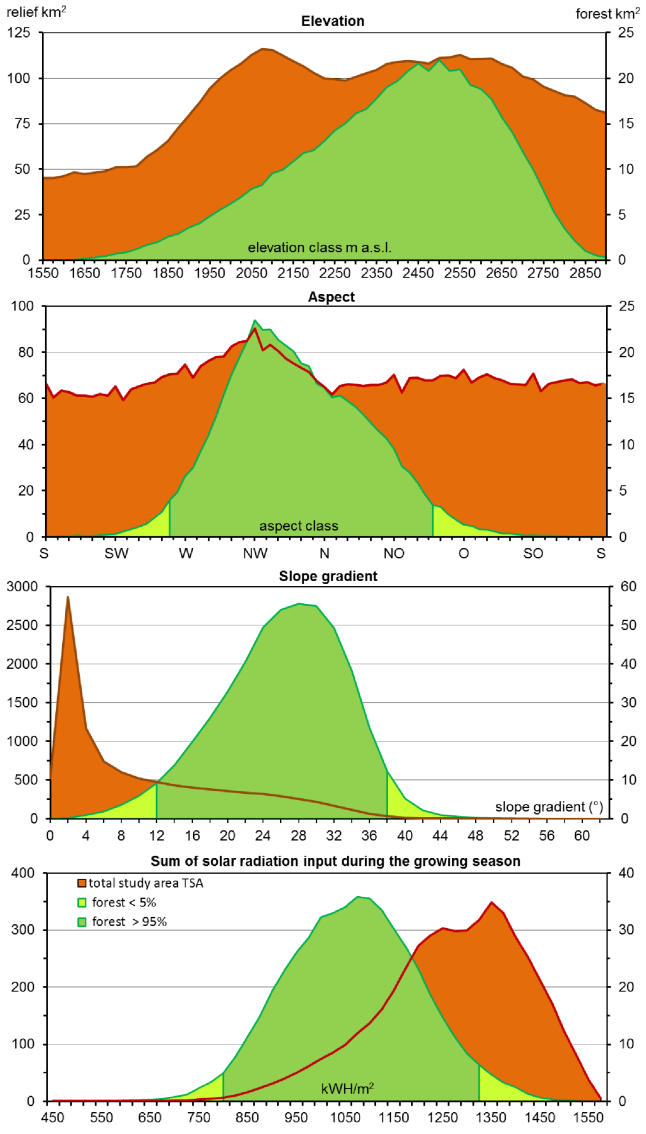


**Figure 4.** Frequency distribution of relief parameters in relation to actual forest area (AFA, green; in the diagrams of aspect, slope gradient and solar radiation input, the light green areas represent the standard deviation of 95 range excluded from PFA delineation) and total study area (TSA, brown).

ber 2000 (Fig. 3). Aerial photos provided as imagery and Bing basemaps by ESRI were used to detect forest area reference sites for the training and validation of the classifier. Two classes were built and manually digitized for the classification and validation process. One class represents the forest areas and the other class includes different kinds of no-forest landscape. Depending on the ground resolution of $30 \times 30$ m, one pixel covers several individual trees so that small clearings and aisles may have been disregarded. The confusion matrix in Table 1 shows a producer's accuracy of 89 % for forest areas, where $\sim 6$ % of the forest area were used for validation. This possible underestimation of the forest area of up to 11 % mainly occurs at the edges of closed forest, where the classification depends on the quantity of trees in one Landsat pixel.

The relief parameters elevation, aspect, slope gradient and total solar radiation input were derived from a DTM based on SRTM data (Rabus et al., 2003), which was converted to UTM zone 44 N with a spatial resolution of $90 \times 90$ m. The polygons of the delineated forest stands were intersected with the relief parameters in order to investigate the relief-dependent spatial distribution of forest sites in the study area. In addition, the statistics of all relief parameters were computed for the total study area (TSA) to indicate the potential impact of topography on the spatial distribution of forest stands (Fig. 4). The PFA was then identified based on the assumption of confidence ranges for all four relief parameters, which were found responsible for forest distribution. This range was defined by the standard deviation (95 % confidence interval) from the single-frequency distribution of the relief parameters aspect, slope gradient and sum of solar radiation input during the mean growing season (March to November). While these parameters are not systematically influenced by human impact, the vertical distribution may have been changed by forest clearing at the lower and upper boundary. Therefore 99 % of the frequency distribution of the elevation parameter was chosen in this case.

Baseline climate data sets for central Asia, comprising monthly radiation, temperature and precipitation data at a horizontal resolution of 0.5 arc seconds (approximately 1200 m in longitudinal and 850 m in latitudinal direction), are provided by Böhner (2006). The regular-grid climate layers were estimated using an empirical modeling approach, which basically integrates statistical downscaling of coarse-resolution atmospheric fields (NCAR/NCEP-CDAS reanalyses series – National Center for Atmospheric Research/National Center for Environmental Prediction – climate data assimilation system; Kalnay et al., 1996) and GIS-based surface parameterization techniques, to sufficiently account for the topographic heterogeneity of the target area. A comprehensive description of data bases and modeling techniques is given in Böhner (2006) and Böhner and Antonic (2009). The suitability and precision of the modeling approach is discussed in Gerlitz et al. (2013, 2014) and Soria-Auza et al. (2010).

The frequency distribution of selected climate parameters related to the AFA and the TSA shown in Fig. 5 was calculated in the same way as described above. In contrast to the high resolution of the SRTM data, the climate data has a resolution about 10 times lower, which leads to a generalization and coarser-scale of relief positions where climatic differences between slope aspects inside the valleys are averaged. The climate data related to the forest stands are analyzed by the climatic limitation values for forest development to detect potential human impact on the forest distribution patterns when obvious discrepancies occur.

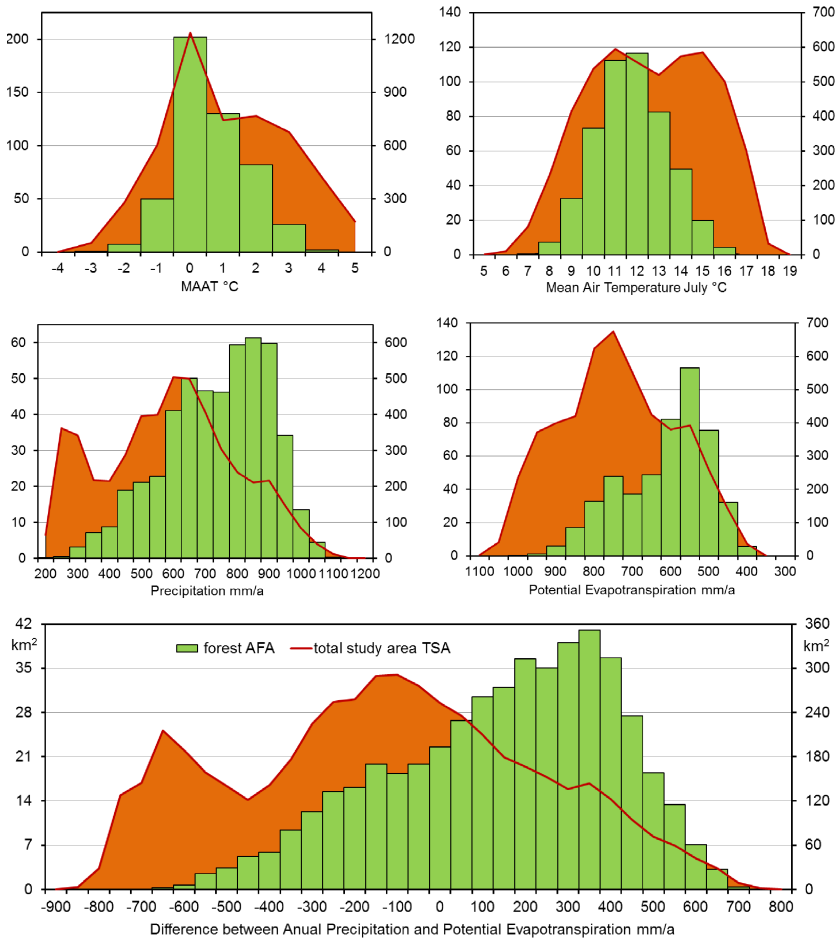


**Figure 5.** Frequency distribution of climate parameters for actual forest area (AFA: columns and left axes, in km$^2$) and the total study area (TSA: graph and right axes, in km$^2$).

**Table 2.** Statistical values of the relief parameters related to the forest distribution.

| Parameter | Unit | Maximum distribution value | Total distribution range | 95 % of the distribution range |
|---|---|---|---|---|
| Elevation | m a.s.l. | 2500 | 1575–2900 | 1925–2775 |
| Aspect | degree horizontal | 315 (NW) | 0–360 | 260–70 |
| Slope gradient | degree vertical | 28 | 0–62 | 12–38 |
| Solar radiation input | kWh m$^{-2}$ | 1075 | 450–1550 | 800–1325 |

To outline the actual forest lines, it is initially necessary to segment the relief into small CAs, which represent small side valleys or slope niches divided by convex ridges. This is done by computing the surficial hydrology regime from the DTM. The size of a CA is given by the threshold value for the stream definition function, which assigns the minimum number of cells that must discharge into a specific cell to start a depth contour. In this study a value of 200 was found practical for the lower forest line and a value of 100 was suitable for the upper forest line. The single CAs generally consist of sections on the left and on the right side of a valley. Having different aspects in one segment is expedient to receive a general forest line value for one valley section.

After combining the catchment polygons with the forest polygons, it is possible to determine the maximum and minimum elevation values for forests inside a single CA. The calculated values are spatially allocated as points to the position of those pixels for which forest line values have been determined. To eliminate the preconditions on the lower forest line given by the elevation limits of the relief, only those

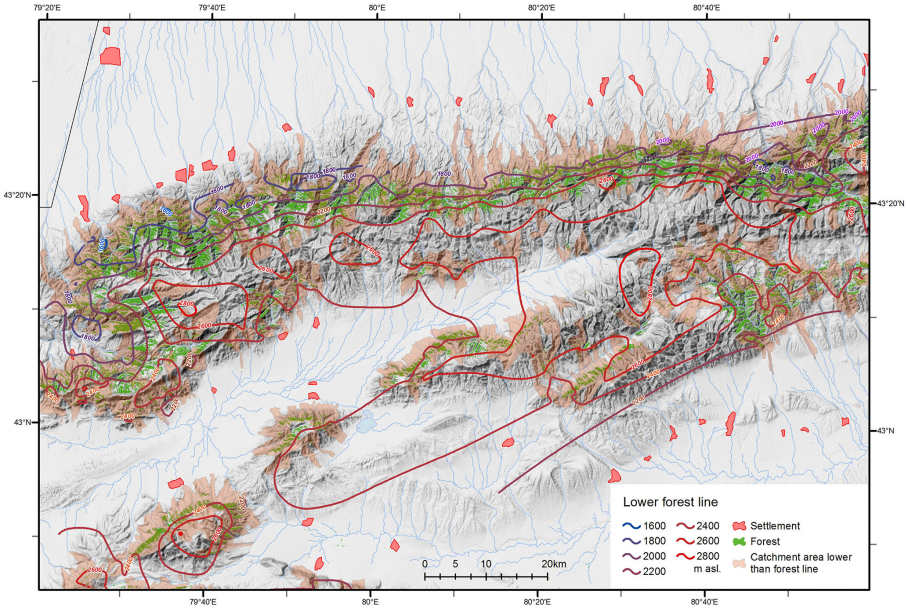


**Figure 6.** The lower forest line and the catchment areas providing lower forest line values in the investigation area.

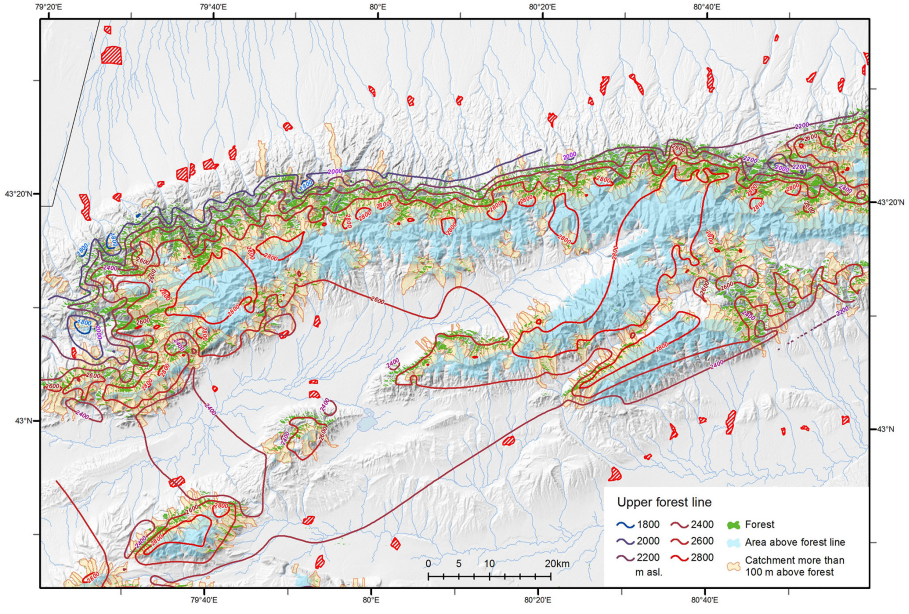


**Figure 7.** The upper forest line and the catchment areas providing upper forest line values in the investigation area.

minimum values of forest stands were chosen which are more than 50 m higher than the total minimum value of the CA. The distance between the highest forest stands and the crest line above has a special influence on the upper forest line; this is called the "summit syndrome" by Körner (2012). Near the summits the local climate conditions strongly suppress tree growth by stronger wind, reduced temperature and snow drift. To receive a reasonable value for the climatic upper forest line and to eliminate preconditions by relief height, only those maximum forest values were chosen which lie more than 100 m below the total maximum elevation of the catchment. Finally, the forest lines were calculated from the remaining points by a Natural Neighbor interpolation method.

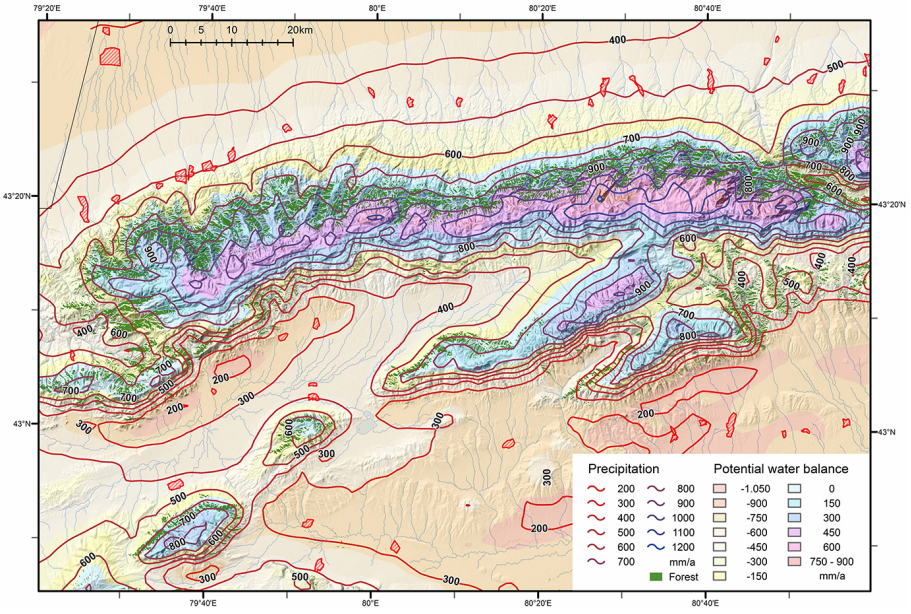


**Figure 8.** Distribution of AFA in relation to the hydrological climatic environment.

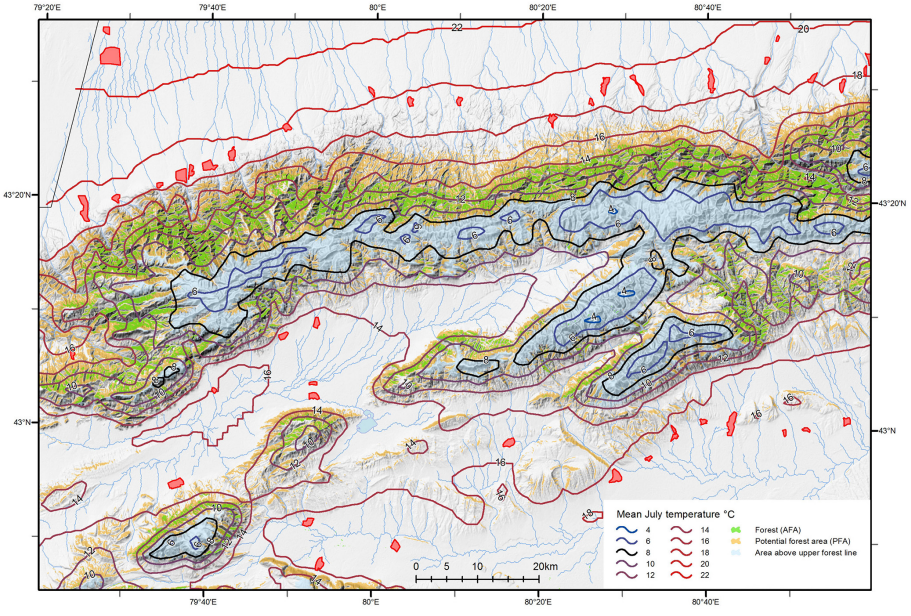


**Figure 9.** Distribution of AFA and PFA and the July isotherms.

## 4 Results

### 4.1 Relief parameterization

The total AFA in the investigation area is 502 km$^2$ (Fig. 3). Frequency distributions of relief parameters for the AFA are shown in Fig. 4. The slope gradient and solar radiation of the forest stands show a normal distribution. The values with the maximum distribution are 28° for slope gradient and 1075 kWh m$^{-2}$ for the sum of solar radiation input (Table 2). Less than 5 % of the forests occur on southern slopes (SE–S–SW). The curve of the parameter aspect has a steeper left slope and a maximum value in the northwestern direction (315°), which is strongly related to the diurnal air temperature trend caused by insolation and heating processes on different slope directions. This underlines the fact that the strong relation of forest distribution to slope aspect is caused by natural environmental conditions. The logistic problems of access in the relief influence how forest is transformed by

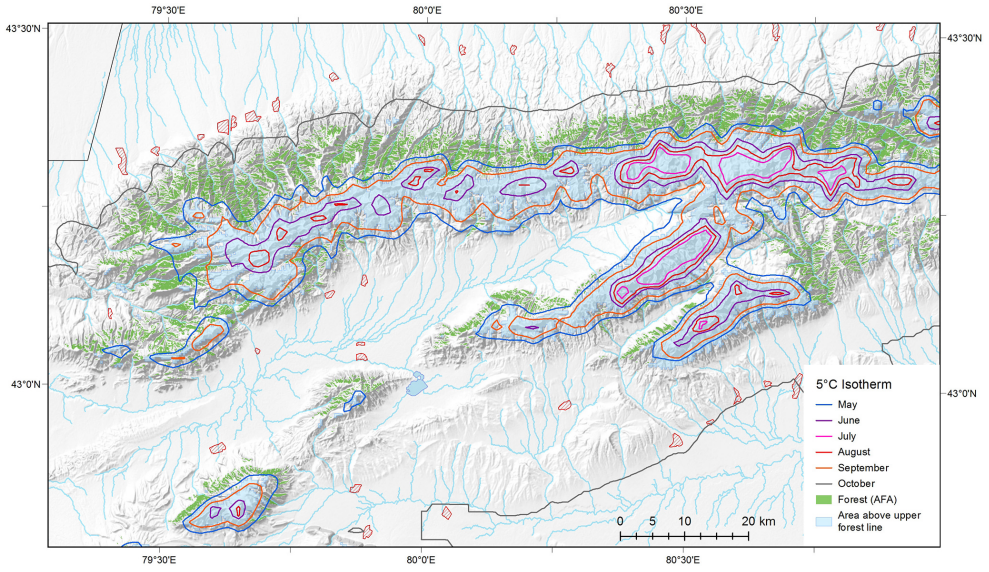


**Figure 10.** Distribution of AFA and the 5 °C monthly isotherms during the growing season

**Table 3.** Comparison between of the modeled area values of single relief parameter classes and of the combination of all four relief parameters. (AFA: actual forest area; PFA: potential forest area.)

| Relief parameter: | Elevation | | | Solar radiation input | | | Slope gradient | | | Slope aspect | | | All four parameters | | |
|---|---|---|---|---|---|---|---|---|---|---|---|---|---|---|---|
| Site classification | km$^2$ | % $FA_{AP}$ | % TMA | km$^2$ | % $FA_{AP}$ | % TMA | km$^2$ | % $FA_{AP}$ | % TMA | km$^2$ | % $FA_{AP}$ | % TMA | km$^2$ | % $FA_{AP}$ | % TMA |
| (3) PFA without AFA | 5358.7 | 91.4 | 65.9 | 4791.2 | 90.5 | 59.0 | 4279.9 | 89.5 | 52.7 | 3850.5 | 88.5 | 47.4 | 1323.6 | 72.5 | 16.3 |
| (1) PFA with AFA | 502.0 | 8.6 | 6.2 | 480.5 | 9.1 | 5.9 | 483.8 | 10.1 | 6.0 | 474.2 | 10.9 | 5.8 | 446.7 | 24.5 | 5.5 |
| (4) No PFA with AFA | 0.3 | 0.004 | 0.003 | 21.5 | 0.4 | 0.3 | 18.0 | 0.4 | 0.2 | 27.9 | 0.6 | 0.3 | 55.4 | 3.0 | 0.7 |
| (2) No PFA without AFA | 2265.2 | | 27.9 | 2832.9 | | 34.9 | 3344.4 | | 41.2 | 3773.6 | | 46.4 | 6300.7 | | 77.5 |
| Sum of all classifications which represent the actual situation | 2767.2 | | 34.1 | 3313.4 | | 40.8 | 3828.3 | | 47.1 | 4247.8 | | 52.3 | 6747.4 | | 83.0 |

% $FA_{AP}$: percentage of the total actual and potential forest area. % TMA: percentage of total mountain area with 8126 km$^2$.

nomads and woodcutters, which reduces the pure signal of elevation in the data. Climate controls environmental conditions in a coarser regional scale and creates sharper elevational boundaries. The curve of the parameter elevation has a shallow left and a steep right slope, which indicates human impact on forest distribution at the lower boundary. The lower forest lines start at 1575 m a.s.l. and the upper forest lines exceed 2900 m a.s.l. so that the maximal vertical distance of the forest limits for the entire investigation area is 1325 m (Table 2).

The TSA represents the complete area of the elevation belt between the forest lines from 1500 and 2900 m a.s.l.. Except for the slope gradient diagram, the flat slope positions $< 5°$ were additionally excluded from the TSA. The resulting TSA is approximately 4975 km$^2$. In regard to the independent frequency distribution curves of the relief parameters in Fig. 4 between forest stands and the TSA, no statistical influence of the main topographic pattern on the forest distribution is detectable.

From a statistical point of view, all four relief parameters control the forest distribution. Therefore, it is necessary to check the modeling accuracy of the PFA received from one single relief parameter against the combination of all four relief parameters (Table 3). Comparing the modeled PFA and the AFA, four different classes can be built: (1) PFA with AFA and (2) no PFA without AFA represent the mapped situation; (3) PFA without AFA and (4) no PFA with AFA represent the differences between modeling and mapping. To receive a statistical background for the evaluation of the modeling quality of the delineated PFA, it is once related to the sum ($FA_{AP}$) of AFA and the PFA and twice referred to the total mountain area (TMA) of 8126 km$^2$, while the boundary between the mountains and the pediments of the foreland is generally defined by the changeover line of the slope gradient at 2.5°. From all four single relief parameters the modeling based on the slope aspect coincides best with the actual situation, but, in any case, the combination of all four parameters obviously enhances the prediction accuracy (Table 3). The PFA calculated from all four relief parameters is 1825 km$^2$ and therefore 3.5 times larger than the AFA. Figure 3 shows the spatial differences between the AFA and PFA. In relation to the AFA the PFA generally extends to the lower and upper elevations.

### 4.2 Forest line patterns

Figure 6 shows the lower forest line in the investigation area starting at 1600 m a.s.l. in the northwest and increasing to 2600 m a.s.l. in the southeast. Values for the lower forest line are mostly derived from the lower CAs but there are also many CAs at the higher elevations of the NFR, where the forest stands do not reach the valley bottom. This phenomenon may be caused by the local relief of tree-free flat valley bottoms, which would be a climate rather than a topographic signal. However, regarding the lower forest line in the second mountain range southeast of the intermountain basin and behind the NFR, it remains at a higher elevation around 2400 m a.s.l.. Here the high lower forest line position is obviously caused by the drier conditions of the rain shadow position, which may also be true for the upper valleys in the NFR.

The upper forest line distribution and the area above the forest line are shown in Fig. 7. In the NFR the upper forest line at the edge of the mountains starts at 1800 m a.s.l. in the west and increases to 2200 m a.s.l. in the east, maintaining a vertical distance of 200 m to the lower forest line. From the edge of the mountains in the north to the crest line, the upper forest line rises to 2800 m a.s.l., and, crossing the intermountain basin, it lies at an elevation between 2400 and 2800 m a.s.l. in the SMR. The local vertical distance of the forest belt reaches its maximum value of more than 900 m on the northern side of the NFR. On the southern side and in the SMR, the forest belt is very narrow, with vertical distances between 50 and 400 m.

### 4.3 Climate environmental conditions

The environmental conditions were analyzed in terms of frequency distribution of climate parameters for the AFA (Fig. 5) and were mapped together with the AFA (Figs. 8–10). The diagrams in Fig. 5 show the differences between AFA and TSA for all climate parameters except for the MAAT, which was already excluded as a significant forest limitation parameter.

The lowest value class of forest stands for annual precipitation is 250 mm, while the highest potential evapotranspiration is up to 1100 mm $a^{-1}$. One third of the AFA lies in areas with a negative potential water balance (pWB, i.e., the difference between annual precipitation and potential evapotranspiration; cf. Fig. 5) but with a precipitation amount of between 300 and 700 mm $a^{-1}$ (Fig. 8). These areas are situated at the westernmost edges and on the southern slopes of the mountain ranges. While the westernmost sites are exposed to the westerlies, which transport most of the humidity, the southern slopes lie in the rain shadow but at a higher elevation, and therefore the lower forest line is around 600 m higher than on the northern side of the NFR.

In the eastern part of the northern side of the NFR, the AFA belt is very small and, concurrently, the lower forest line increases to 2000 m a.s.l., 400 m higher than in the western part of the NFR. Here, the lower forest line occurs with a precipitation of 700 mm and at a positive pWB of 150 to 300 mm $a^{-1}$, while the PFA extends more into the lower slope positions; this corresponds to the mean values of the regions described above. This is an indication for a nonnatural distribution and points to greater human influence on forests in this region.

The forest distribution related to mean air temperature in July ranges between 7 and 17 °C, with a maximum of around 11 to 12 °C (Fig. 5). Comparing the AFA and PFA with the July isotherms (Fig. 9) shows that the upper AFA is mainly bordered by the 10 °C July isotherm but also extends to the 8 °C July isotherm in many places. The upper PFA is generally aligned to the 8 °C July isotherm. Figure 10 shows the distribution of the monthly mean air temperature 5 °C isotherm during the growing season and the AFA. Except at the westernmost part, the 5 °C isotherm is above the AFA between June and September, and the upper AFA boundary coincides well with the 5 °C isotherm of September. The PFA at the upper forest boundary extends up to the position of 5 °C isotherm in June; the growing season obviously becomes very short at these highly elevated places. As shown in Figs. 9 and 10, the PFA at the upper limit is overestimated and the upper AFA boundary generally has a natural limitation.

## 5 Discussion and conclusions

It was shown that the AFA and the forest lines coincide well with the local climate conditions. At the lower limit, forests are restricted to a minimum annual precipitation of 250 mm. The upper forest line coincides with the 10 °C July isotherm in most places and to the minimum monthly mean temperature of 5 °C for the period between June and September. In the more humid parts of the investigation area at the western and northern slopes of the NFR both forest lines have a steep gradient and the forest belt has its greatest vertical extension between 500 and 600 m and locally up to 900 m. This agrees well with the findings of increasing vertical forest extension concurrent with increasing humidity and vice versa by Fickert (1998), Dai et al. (2013) and Klinge et al. (2003) in the surrounding regions. Besides temperature, rainfall influences the upper forest line because clouds reduce the air temperature by shadowing and by the reflection of solar insulation. This explains the steep gradient of the upper forest line at the windward side of the mountain ridges.

The comparison of the AFA with climate data reveals a strong relation between the distribution patterns at the upper boundary, but divergences occur at the lower boundary. This indicates human impact on the forests at the edge of the mountains, modifying the lower forest line, while the upper forest line represents the natural condition. Accordingly the PFA derived from relief parameters at lower elevations in-

dicates additional area for more potential natural forest. The PFA at the upper boundary is overestimated by highest forest stands occurring at few places with favorable climatic conditions because we used the total vertical distance of forest distribution as a relief parameter instead of the standard variation, presuming that extensive logging may also occur in the alpine meadow pastures. GIS analysis combined with multispectral satellite images and DTM is well suited to determine forest lines and potential forest areas for semiarid regions on a local to regional scale. For forest line delineation it is necessary to eliminate elevation values which are restricted by the relief conditions and do not represent climatic limitations. The DTM-derived relief parameters slope aspect, gradient and solar radiation serve well as indicators of the climatic environment in the investigation area and help to transfer environmental settings to other places in the broader study area. Human impact is recognized by the evaluation of the parameter elevation. Therefore, a forest line evaluation with respect to the general climatic conditions has to be performed before the parameter elevation is incorporated into the spatial delineation process of the PFA. In conclusion, the proposed workflow is a helpful method for the evaluation of the potential forest distribution and the delineation of human impact. It can be used to indicate local climate variability, for landscape analysis and for effective reforestation planning.

*Acknowledgements.* The authors would like to thank the US Geological Survey for making the satellite data freely available for scientific research. We acknowledge support by the Open Access Publication Funds of Göttingen University. We also thank F. Lehmkuhl and two anonymous referees for their great support in improving the manuscript of this publication.

This open-access publication was funded
by the University of Göttingen.

Edited by: A. Ito

## References

Böhner, J.: General climatic controls and topoclimatic variations of Central and High Mountain Asia, Boreas, 35, 279–295, 2006.

Böhner, J. and Antonic, O: Land-Surface Parameters Specific to Topo-Climatology, in: Geomorphometry: Concepts, Software, Applications, edited by: Hengl, T. and Reuter, H. I., Dev. Soil Science, 33, 195–226, 2009.

Dai, L., Li, Y., Luo, G., Xu, W., Lu, L., Li, C., and Feng, Y.: The spatial variation of alpine timberlines and their biogeographical characteristics in the northern Tianshan Mountains of China, Environ. Earth Sci., 68, 129–137, 2013.

Dulamsuren, C., Hauck, M., Khishigjargal, M., Leuschner, H. H., and Leuschner, C.: Diverging climate trends in Mongolian taiga forests influence growth and regeneration of Larix sibirica, Oecologia, 63, 1091–1102, 2010.

Dulamsuren, C., Khishigjargal, M., Leuschner, C., and Hauck, M.: Response of tree-ring width to climate warming and selective logging in larch forests of the Mongolian Altai, J. Plant Ecol., 7, 24–38, 2014.

Fickert, T.: Vergleichende Beobachtungen zu Solifluktions- und Frostmustererscheinungen im Westteil Hochasiens, Erlanger Geogr. Arb., 60, 150 pp., 1998.

Gerlitz, L., Bechtel, B., Zaksek, K., Kawohl, T., and Böhner, J.: SAGA GIS based processing of spatial high resolution temperature data, Proceedings of the 27th EnviroInfo-Conference, 2013, 693–702, 2013.

Gerlitz, L., Conrad, O., Thomas, A., and Böhner, J.: Assessment of Warming Patterns for the Tibetan Plateau and its adjacent Lowlands based on an elevation and bias corrected ERA-Interim Data Set, Climate Res., 58, 235–246, 2014.

Giese, E.: Wetterwirksamkeit atmosphärischer Zustände und Prozesse in Sowjet-Mittelasien, Westfälische Geogr. Stud., 37, 395–410, 1973.

Giese, E.: Seßhaftwerden von Nomaden, Erfahrungen über die Dynamik traditioneller sozialer Einrichtungen (am Beispiel des kasachischen Volkes), in: Die Nomaden in Geschichte und Gegenwart, Beiträge zu einem internationalen Nomadismus-Symposium am 11 und 12 Dezember 1975 im Museum für Völkerkunde Leipzig, Berlin, 175–197, 1981.

Giese, E.: Nomaden in Kasachstan – Ihre Seßhaftwerdung und Einordnung in das Kolchos- und Sowchossystem, Geogr. Rundschau, 11, 575–588, 1983.

Haase, G., Richer, H., and Barthel, H.: Zum Problem landschaftsökologischer Gliederung, dargestellt am Beispiel des Changai-Gebirges in der Mongolischen Volksrepublik, Wiss. Veröff. Deutschen Inst. Länderk., 21/22, 489–516, 1964.

Hansen, M. C., Potapov, P. V., Moore, R., Hancher, M., Turubanova, S. A., Tyukavina, A., Thau, D., Stehman, S. V., Goetz, S. J., Loveland, T. R., Kommareddy, A., Egorov, A., Chini, L., Justice, C. O., and Townshend, J. R. G.: High-Resolution Global Maps of 21st-Century Forest Cover Change, Science, 342, 850–853, 2013.

Hilbig, W.: The Vegetation of Mongolia, Amsterdam, 258 pp., 1995.

Holdridge, L. R.: Determination of world plant formations from simple climatic data, Science, 105, 367–368, 1947.

Holtmeier, F.-K.: Die Höhengrenze der Gebirgswälder, Arb. Inst. Landschaftsökologie, 8, 337 pp., 2000.

Hövermann, J.: Das System der klimatischen Geomorphologie auf landschaftskundlicher Grundlage, Z. Geomorphol. N. F., Supp., 56, 143–153, 1985.

Jobbagy, E. G. and Jackson, R. B.: Global controls of forest line elevation in the northern and southern hemispheres, Global Ecol. and Biogeogr., 9, 253–268, 2000.

Kalnay, E., Kanamitsu, M., Kistler, R., Collins, W., Deaven, D., Gandin, L., Iredell, M., Saha, S., White, G., Woollen, J., Zhu, Y., Leetmaa, A., Reynolds, R., Chelliah, M., Ebisuzaki, W., Higgins, W., Janowiak, J., Mo, K. C., Ropelewski, C., Wang, J., Jenne, R., and Joseph, D.: The NCEP/NCAR 40-year reanalysis project, Bull. Amer. Meteor. Soc., 77, 437–470, 1996.

Karger, A.: Historisch-geographische Wandlungen der Weidewirtschaft in den Trockengebieten der Sowjetunion am Beispiel Kasachstans, in: Weide-Wirtschaft in Trockengebieten, edited by: Knapp, R., Gießen, 37–49, 1965.

Kastner, M.: Patterns of forest distribution in Western Mongolia, Berliner Geowissensch. Abh., 205, 67–71, 2000.

Klinge, M., Böhner, J., and Lehmkuhl, F.: Climate patterns, snow- and timberlines in the Altai Mountains, Central Asia, Erdkunde, 57, 296–308, 2003.

Körner, C.: Alpine Treelines, Functional Ecology of the Global High Elevation Tree Limits, Springer, Basel, 220 pp., 2012.

Körner, C. and Paulsen, J.: A world-wide study of high altitude treeline temperatures, J. Biogeogr., 31, 713–732, 2004.

Liang, E., Lu, X., Ren, P., Li, X., Zhu, L., and Eckstein, D.: Annual increments of juniper dwarf shrubs above the tree line on the central Tibetan Plateau: a useful climatic proxy, Ann. Bot.-London, 109, 721–728, 2012.

Liu, H., Williams, A. P., Allen, C. D., Guo, D., Wu, X., Anenkhonov, O. A., Liang, E., Sandanov, D. V., Yin, Y., Qi, Z., and Badmaeva, N. K.: Rapid warming accelerates tree growth decline in semi-arid forests of Inner Asia, Glob. Change Biol., 19, 2500–2510, 2013.

Lydolph, P. E.: Climates of the Soviet Union, World Survey of Climatology, 7, Amsterdam, 443 pp., 1977.

Machalett, B., Frechen, M., Hambach, U., Oches, E. A., Zöller, L., and Markovic, S. B.: The loess sequence from Remisowka (northern boundary of the Tien Shan Mountains, Kazakhstan) - Part I: Luminescence dating, Quaternary Int., 152/153, 192–201, 2006.

Mayer, T. and Bussemer, S.: Die Waldsteppe Südsibiriens. Ökosystemanalyse mit Hilfe der Radarfernerkundung, Mitt. Geogr. Gesell. München, 85, 161–180, 2001.

Medeu, A. R.: The national atlas of the Republic of Kazakhstan / Institute of Geography, Part 1: Natural conditions and resources, Almaty, 2010, 150 pp., 2010.

Miehe, G. and Miehe, S.: Comparative high mountain research on the treeline ecotone under human impact, Erdkunde, 54, 34–50, 2000.

Miehe, G., Miehe, S., Koch, K., and Will, M.: sacred forests in Tibet – using geographical information systems for forest rehabilitation, Mt. Res. Dev., 23, 324–328, 2003.

Miehe, G., Miehe, S., Will, M., Opgenoorth, L., Duo, L., Dorgeh, T., and Liu, J.: An inventory of forest relicts in the pastures of Southern Tibet, editd by: Xizang, A. R., China, Plant Ecol., 194, 157–177, 2008.

Paulsen, J. and Körner, C.: A climate-based model to predict potential treeline position around the globe, Alpine Botany, 124, 1–12, 2014.

Rabus, B., Eineder, M., Roth, A., and Bamler, R: The shuttle radar topography mission – a new class of digital elevation models acquired by spaceborne radar, ISPRS J. Photogramm., 57, 241–262, 2003.

Schlütz, F., Dulamsuren, C., Wieckowska, M., Mühlenberg, M., and Hauck, M.: Late Holocene vegetation history suggests natural origin of steppes in the northern Mongolian mountain taiga, Palaeogeogr. Palaeocl., 261, 203–217, 2008.

Soria-Auza, R. W., Kessler, M., Bach, K., Barajas-Barbosa, P. M., Lehnert, M., Herzog, S. K., and Böhner, J.: Impact of the quality of climate models for modelling species occurrences in countries with poor climatic documentation: a case study from Bolivia, Ecol. Model., 221, 1221–1229, doi:10.1016/j.ecolmodel.2010.01.004, 2010.

Treter, U.: Gebirgs-Waldsteppe in der Mongolei, Geogr. Rundschau, 48, 655–661, 1996.

Treter, U.: Recent extension and regeneration of the larch forest in the mountain forest steppe of north-west Mongolia, Marburger Geogr. Schriften, 135, 156–170, 2000.

Troll, C.: The upper timberlines in different climate zones, Arctic Alpine Res., 5, A3–A18, 1973a.

Troll, C.: High mountain belts between the polar caps and the equator: Their definition and lower limit, Arctic Alpine Res., 5, A19–A27, 1973b.

von Humboldt, A.: Kosmos: Entwurf einer physischen Weltbeschreibung, Stuttgart, 5 volumes, 1847–1862.

Walter, H. and Breckle, S. W.: Spezielle Ökologie der Gemäßigten und Arktischen Zonen Euro-Nordasiens, Ökologie der Erde, 3, Jena, 726 pp., 1994.

Wang, T., Ren, H., and Ma, K.: Climatic signals in tree ring of Picea schrenkiana along an altitudinal gradient in the central Tianshan Mountains, northwestern China, Trees, 19, 735–741, 2005.

Wang, T., Zhang, Q. B., and Ma, K.: Treeline dynamics in relation to climatic variability in the central Tianshan Mountains, northwestern China, Global Ecol. Biogeogr., 15, 406–415, 2006.